Supplementary Information (SI) for Chemical Science.
This journal is © The Royal Society of Chemistry 2024

Supporting Information

Unique trimeric triphenylene radical cation: Stacking aggregation, bonding, and stability

Rameswar Bhattacharjee,[1] Megan E. McCormack,[2] Zheng Zhou,[2,3] Zheng Wei,[2]

Marina A. Petrukhina[2,*] Miklos Kertesz,[1,*]

[1]Department of Chemistry and Institute of Soft Matter, Georgetown University

37th and O Streets, NW, Washington, DC 20057-1227, USA

[2]Department of Chemistry, University at Albany, State University of New York, 1400 Washington Avenue, Albany, NY 12222, USA

[3]School of Materials Science and Engineering, Tongji University, 4800 Cao'an Road, Shanghai 201804, China

Table of Contents

I. Materials and methods 3

II. Crystal structure solution and refinement 4

III. Comparison of different gallium(III) chlorides 12

IV. Characterization of $(C_{18}H_{12})_3^{\bullet+}(Ga_3Cl_{10})^-$ 13

V. Computational methods 17

VI. Validation of Charge Distributions in $[(C_{18}H_{12})_3]^{+1}$ 19

VII. Size dependency of the interaction energy in π*-stacking aggregates of TP cation radical columns* 19

VIII. HOMA analysis 20

IX. Bond distance distribution in various positively charged TP cation radical aggregates 21

X. The effect of different isovalues for illustrating intermolecular overlap 22

XI. References 23

I. Materials and methods

All manipulations were carried out using break-and-seal[1] and glove-box techniques under an atmosphere of argon. Fluorobenzene (99%) was dried over 4 Å molecular sieves and degassed. Triphenylene (>96%) was purchased from TCI America and purified through sublimation at 185°C prior to use. Gallium (III) chloride (ultra dry ≥99.999%) was purchased from Thermo Scientific and used as received. The UV-vis absorption spectra were recorded on a Shimadzu 2600i UV-visible Spectrophotometer. The EPR spectrum was recorded on a LINEV ADANI Spinscan X Electron Paramagnetic Resonance Spectrometer. Powder X-ray diffraction data were collected on a Bruker VENTURE system equipped with a PHOTON 100 CMOS detector, a Mo-target fine-focus X-ray source (λ = 0.71073 Å), and a graphite monochromator at 100(2) K. The IR spectrum was collected on a Shimadzu IRTracer-100 Fourier Transform Infrared Spectrometer QATR10 Single Reflection ATR accessory.

Preparation of $(C_{18}H_{12})_3^{\bullet+}(Ga_3Cl_{10})^-$

Anhydrous fluorobenzene (2.0 mL) was added to a custom-built glass system containing triphenylene (10.0 mg, 0.0438 mmol) and $GaCl_3$ (11.4 mg, 0.0659 mmol). The mixture was allowed to stir under argon at 40°C for 90 minutes in a closed system. The initial suspension was a pale orange-pink and changed to a bright pink after 2 minutes. The suspension was filtered, the bright pink filtrate was sealed in an L-shaped ampule. The ampule was placed over a sand bath at 40°C. Dark purple blocks were deposited after two weeks. Yield: 11.3 mg, 42%. ATR-IR: 418, 617, 731, 1432, 1497, 3043 cm^{-1}.

II. Crystal structure solution and refinement

Data collection of $[(C_{18}H_{12})_3]^{\bullet+}(Ga_3Cl_{10})^-$ was performed on a Bruker VENTURE system equipped with a PHOTON 100 CMOS detector, a Mo-target fine-focus X-ray source (λ = 0.71073 Å), and a graphite monochromator. The data were collected at 100(2) K crystal temperature (Oxford Cryosystems CRYOSTREAM 700) with an appropriate 0.5° ω scan strategy. The dataset's reduction and integration were performed with the Bruker software package SAINT (version 8.38A).[2] Data were corrected for absorption effects using the empirical methods as implemented in SADABS (version 2016/2).[3] The structure was solved by SHELXT (version 2018/2)[4] and refined by full-matrix least-squares procedures using the SHELXTL (version 2019/2)[5] software through the OLEX2 graphical interface.[6] All non-hydrogen atoms were refined anisotropically. Hydrogen atoms were included in idealized positions for structure factor calculations with U_{iso}(H) = 1.2 U_{eq}(C). The structure was refined as an inversion twin with the BASF value refined to 0.03872. Further crystal and data collection details are listed in Table S1. The ORTEP drawings and additional structural figures, along with the key C–C bond distances and angles, are shown below.

Table S1 Crystal data and structure refinement parameters for $[(C_{18}H_{12})_3]^{\bullet+}(Ga_3Cl_{10})^-$.

Compound	$[(C_{18}H_{12})_3]^{\bullet+}(Ga_3Cl_{10})^-$
Empirical formula	$C_{54}H_{36}Cl_{10}Ga_3$
Formula weight	1248.49
Temperature (K)	100(2)
Wavelength (Å)	0.71073
Crystal system	Monoclinic
Space group	$P2_1$
a (Å)	12.5889(11)
b (Å)	15.8207(13)
c (Å)	12.6280(11)
α (°)	90.00
β (°)	94.562(2)
γ (°)	90.00
V (Å^3)	2507.1(4)
Z	2
ρ_{calcd} (g·cm^{-3})	1.654
μ (mm^{-1})	2.172
F(000)	1246
Crystal size (mm)	0.02×0.16×0.20
θ range for data collection (°)	3.041-27.947
Reflections collected	69249
Independent reflections	12006 [R_{int} = 0.0475]
Transmission factors (min/max)	0.5388/0.7317
Data/restraints/params.	12006/1/605
$R1$,[a] $wR2$[b] ($I > 2\sigma(I)$)	0.0315, 0.0641
$R1$,[a] $wR2$[b] (all data)	0.0407, 0.0674
Quality-of-fit[c]	1.034

$R_{int} = \Sigma|F_o^2-\langle F_o^2\rangle|/\Sigma|F_o^2|$

[a]$R1 = \Sigma||F_o|-|F_c||/\Sigma|F_o|$. [b]$wR2 = [\Sigma[w(F_o^2-F_c^2)^2]/\Sigma[w(F_o^2)^2]]$.

[c]Quality-of-fit = $[\Sigma[w(F_o^2-F_c^2)^2]/(N_{obs}-N_{params})]^{1/2}$, based on all data.

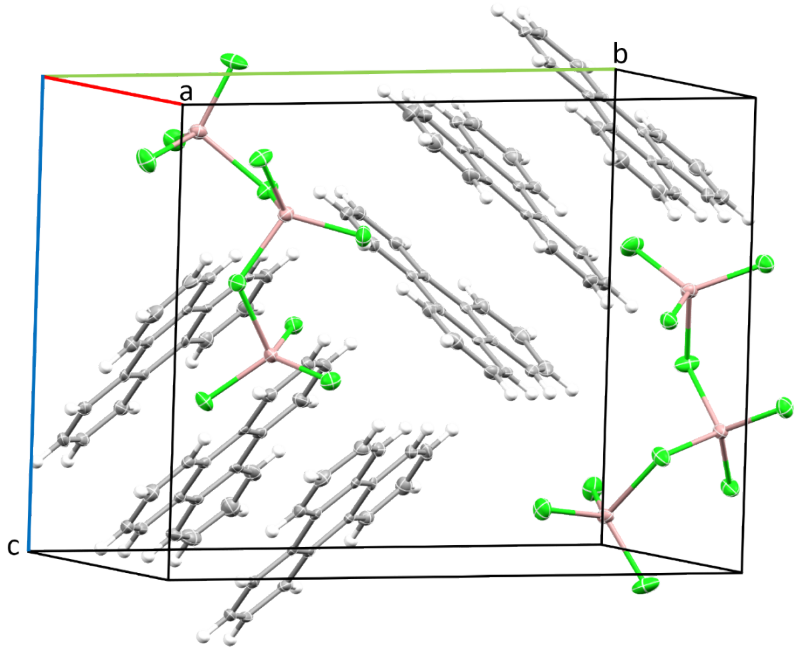

Fig. S1 Unit cell of $[(C_{18}H_{12})_3]^{\bullet+}(Ga_3Cl_{10})^-$, ORTEP drawing with thermal ellipsoids shown at the 50% probability level.

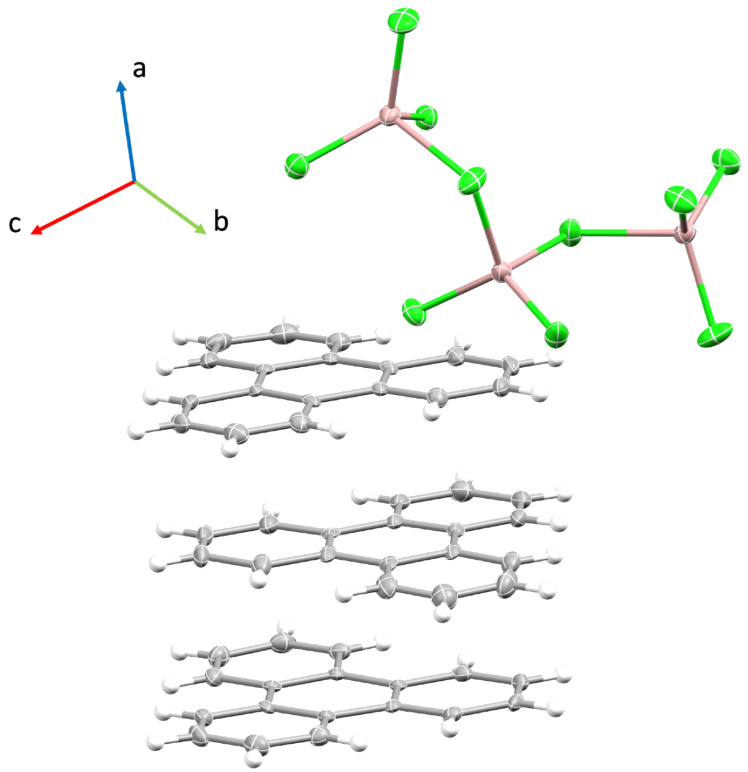

Fig. S2 ORTEP drawing of the asymmetric unit of $[(C_{18}H_{12})_3]^{\bullet+}(Ga_3Cl_{10})^-$ with thermal ellipsoids shown at the 50% probability level.

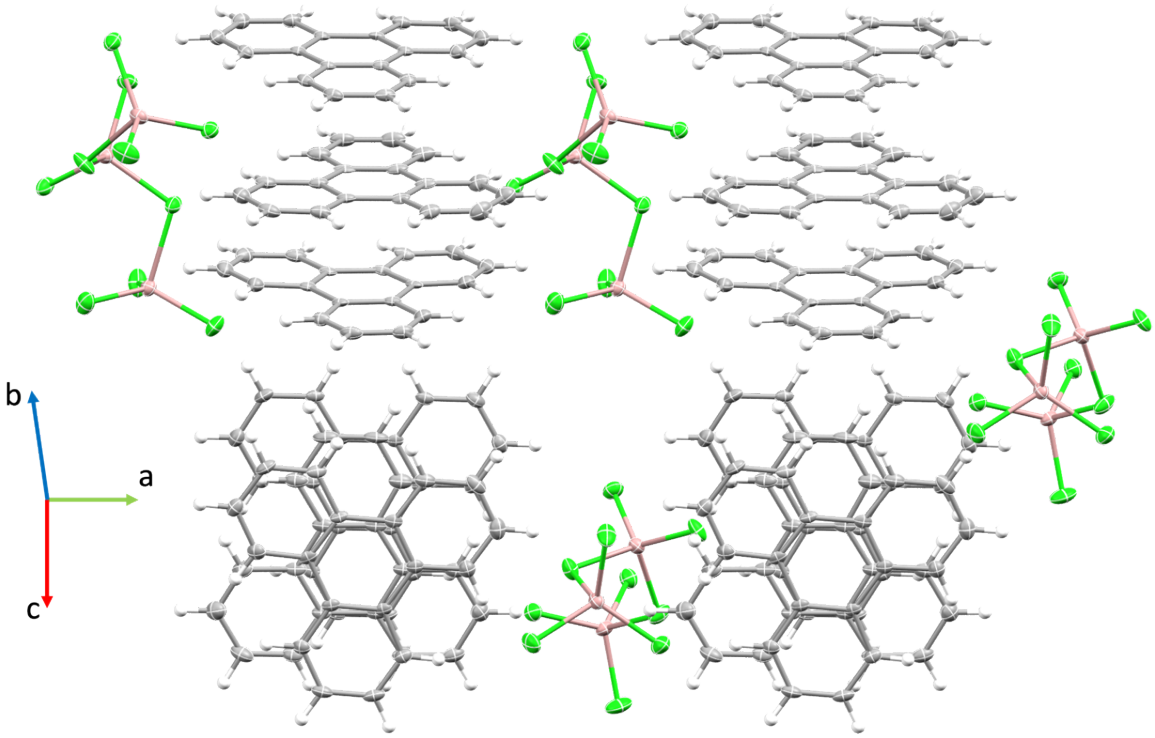

Fig. S3 Solid-state packing of $[(C_{18}H_{12})_3]^{\bullet+}(Ga_3Cl_{10})^-$, ORTEP drawing with thermal ellipsoids shown at the 50% probability level.

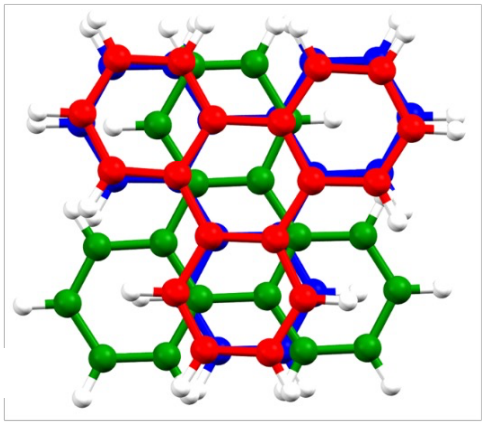

Fig. S4 Surface overlap of neighboring triphenylene molecules. The three molecules in the trimer are in a π-stacking configuration in the order of blue, green, and red.

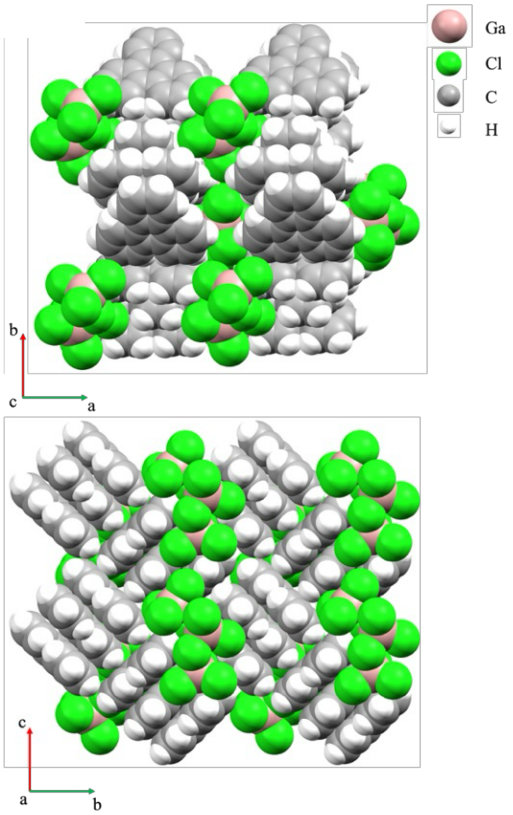

Fig. S5 Solid-state packing of $(C_{18}H_{12})_3^{\bullet+}(Ga_3Cl_{10})^-$ along the *c*- and *a*-axis, space-filling model.

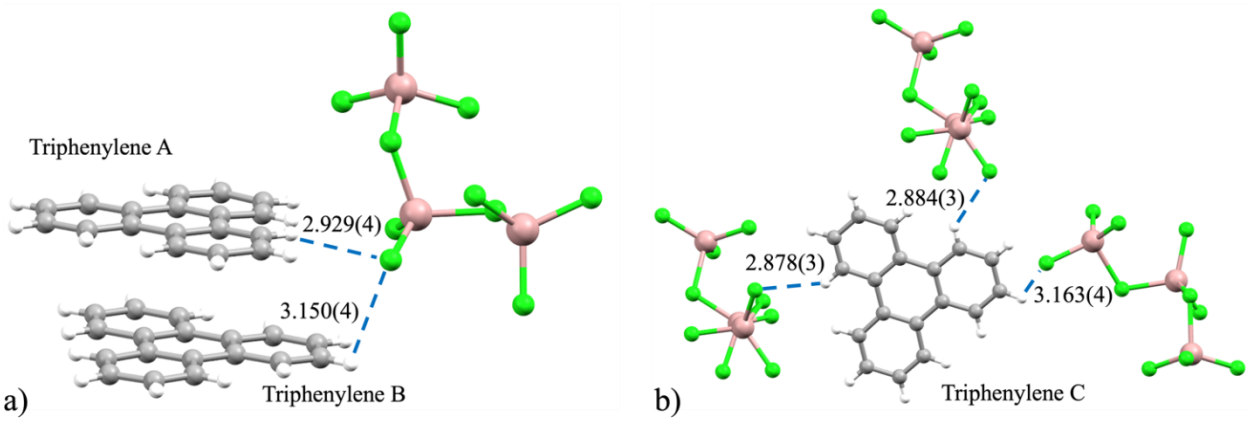

Fig. S6 (a) H···Cl bonding interactions with triphenylene A and B, (b) H···Cl bonding interactions with triphenylene C.

Table S2 Selected C-C bond lengths of crystallographically independent triphenylene molecules, along with a labeling scheme.

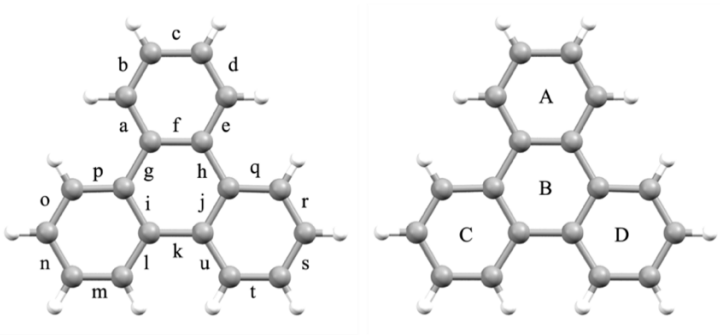

Bond	Neat Triphenylene (Å)	Triphenylene A (Å)	Triphenylene B (Å)	Triphenylene C (Å)
a	1.411(4)	1.416(6)	1.410(6)	1.398(5)
d	1.384(5)	1.371(6)	1.367(6)	1.382(5)
e	1.404(4)	1.402(7)	1.417(6)	1.405(6)
f	1.464(4)	1.409(6)	1.423(6)	1.410(6)
h	1.470(4)	1.466(7)	1.436(7)	1.462(5)
j	1.405(5)	1.413(6)	1.404(6)	1.420(5)
n	1.376(4)	1.389(6)	1.398(7)	1.393(5)
o	1.378(4)	1.371(6)	1.364(6)	1.374(6)
q	1.406(4)	1.406(7)	1.477(6)	1.405(5)
r	1.384(4)	1.359(6)	1.456(7)	1.377(5)
s	1.385(4)	1.396(6)	1.350(6)	1.391(5)
t	1.376(5)	1.372(6)	1.409(6)	1.366(5)

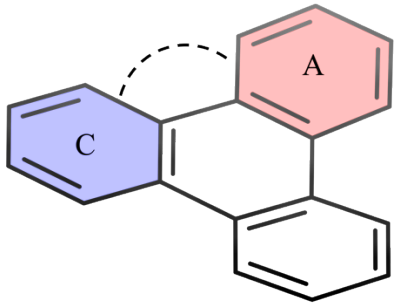

Scheme S1 Determination of selected angles in triphenylene: the angle is measured between planes of each ring face.

Table S3 Selected dihedral angles (°) of triphenylene.

Ring	Neat Triphenylene	Triphenylene A	Triphenylene B	Triphenylene C
A/D	2.68°	2.91°	1.50°	0.97°
A/B	1.32°	2.36°	1.54°	1.76°
A/C	1.99°	3.43°	2.72°	2.74°

III. Comparison of different gallium(III) chlorides

The earliest reports of the $Ga_3Cl_{10}^-$ anion determine composition through Raman spectroscopy[7] and ^{71}Ga NMR spectroscopy.[8,9,10] The first crystallographic "chain-shaped" $Ga_3Cl_{10}^-$ anion (Scheme S2a) is observed in the single crystals of $[Pt_2Ga_2Cl_2(\mu\text{-}Cl)_2(chrysene)_4](Ga_3Cl_{10})_2$, prepared through a reaction of platinum(II) and gallium (III) chlorides with chrysene.[11] This work was followed by the crystallographic determination of a "star-shaped" $Ga_3Cl_{10}^-$ (Scheme S2b), where three $GaCl_3$ units are linked through a central chloride in the single crystals of $[Bi_3GaS_5]_2[Ga_3Cl_{10}]_2[GaCl_4]_2\cdot S_8$.[12] Most recently, this anion is observed through the formation of a dicationic germapyramidane with both $Ga_2Cl_7^-$ and $Ga_3Cl_{10}^-$.[13] A more pronounced bend of the anionic chain (113.07°) is observed in the crystal structure of this work, $(C_{18}H_{12})_3^{\bullet+}(Ga_3Cl_{10})^-$, in comparison to the previously reported "chain-shaped" $Ga_3Cl_{10}^-$ (155.30°).[11]

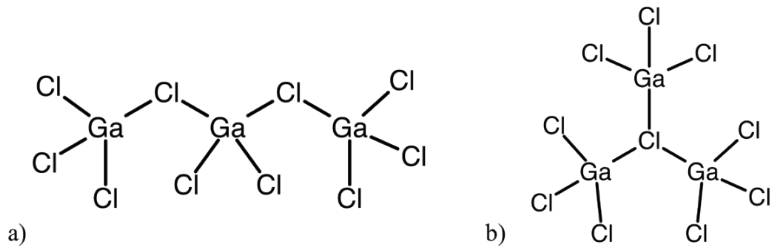

Scheme S2 (a) "Chain-shaped" $Ga_3Cl_{10}^-$ anion,[11] and (b) "star-shaped" $Ga_3Cl_{10}^-$.[12]

IV. Characterization of $(C_{18}H_{12})_3^{\bullet+}(Ga_3Cl_{10})^-$

UV-vis Spectroscopy

Sample Preparation: Several dark purple blocks of $(C_{18}H_{12})_3^{\bullet+}(Ga_3Cl_{10})^-$ (0.2 mg) were dissolved in fluorobenzene (1.5 mL). Separately, triphenylene (0.2 mg) was dissolved in fluorobenzene (1.5 mL). The ampules were sealed under argon and UV-Vis absorption spectra were recorded at 25°C. No spectral changes were detected in comparison to neat triphenylene solution, despite visible changes in the solution color from colorless to a pale pink, indicating disruption of the triphenylene π-stacks in solution.

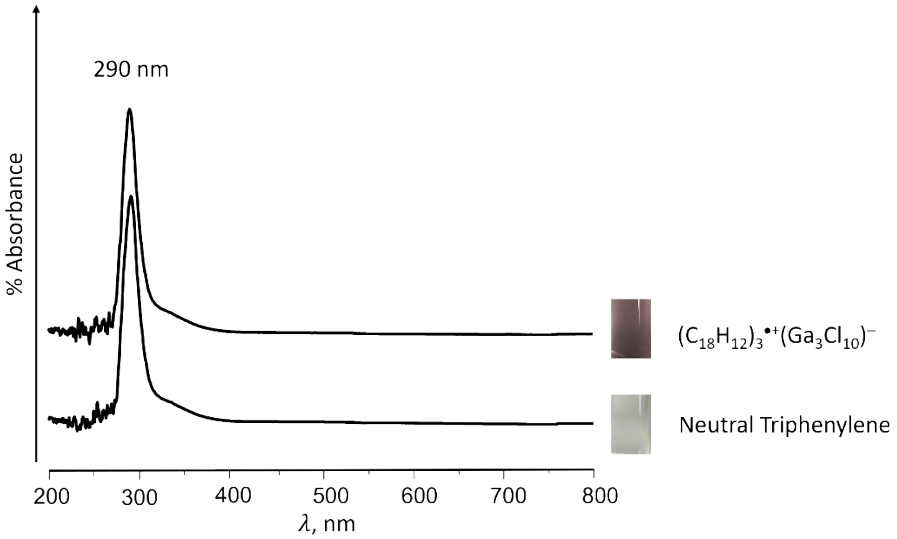

Fig. S7 UV-Vis absorption spectra of the $(C_{18}H_{12})_3^{\bullet+}(Ga_3Cl_{10})^-$ crystals dissolved in fluorobenzene. The spectrum was collected on a Thermo Scientific Evolution 201 UV-Visible Spectrophotometer.

EPR Spectroscopic Investigation

Sample Preparation: Crystals of $(C_{18}H_{12})_3^{\bullet+}(Ga_3Cl_{10})^-$ were moved into the glovebox to remove the pale pink solution. The crystalline material (1.0 mg) was dried *in-vacuo* and loaded into a quartz capillary tube (O.D. 1.25 mm). The tube was sealed and EPR spectrum was collected at 31.9°C (Fig. 3).

X-ray Powder Diffraction

Sample Preparation: Powder X-ray diffraction was performed on the bulk crystalline sample of $(C_{18}H_{12})_3^{\bullet+}(Ga_3Cl_{10})^-$. The purple plates were ground with a small amount of mineral oil under inert atmosphere, and no evidence of decomposition was observed. The powder diffraction pattern of $(C_{18}H_{12})_3^{\bullet+}(Ga_3Cl_{10})^-$ was collected at room temperature to show a good fit with the calculated Le Bail fit (Table S4 below), thus confirming the phase purity of the bulk crystalline sample.

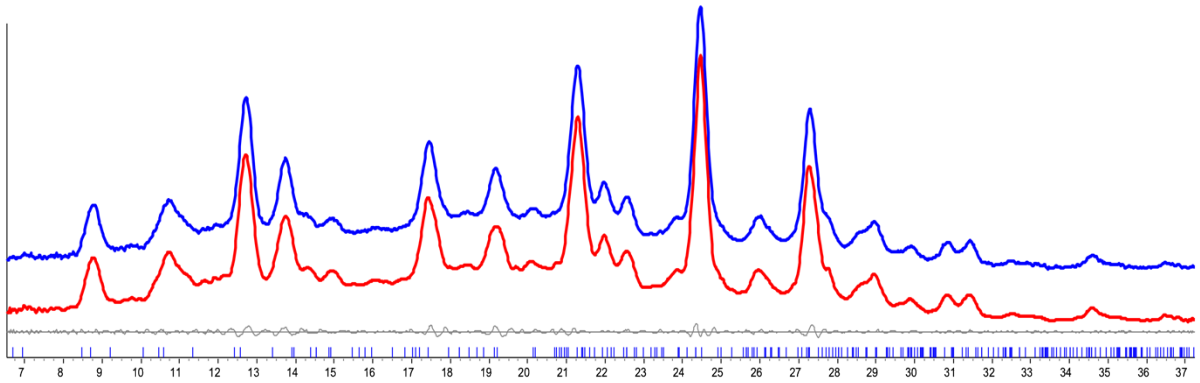

Fig. S8 Experimental Powder X-ray diffraction of $(C_{18}H_{12})_3^{\bullet+}(Ga_3Cl_{10})^-$ (blue line) with Le Bail fit (red line).

Table S4 Single crystal and Le Bail fit data of $(C_{18}H_{12})_3^{\bullet+}(Ga_3Cl_{10})^-$.

$[(C_{18}H_{12})_3]^{\bullet+}(Ga_3Cl_{10})^-$		
	Single crystal data (100 K)	Le Bail fit data (100 K)
Space Group	$P2_1$	
a (Å)	12.5889(11)	12.5874(15)
b (Å)	15.8207(13)	15.8192(16)
c (Å)	12.6280(11)	12.6290(15)
α (°)	90.00	90.00
β (°)	94.562(2)	94.558(4)
γ (°)	90.00	90
V (Å3)	2507.1(4)	2506.8(6)

ATR-IR Spectroscopy

Sample Preparation: Dark purple crystals of $(C_{18}H_{12})_3^{\bullet+}(Ga_3Cl_{10})^-$ were washed with hexanes (2.0 mL) and dried *in-vacuo*. The crystals (5.0 mg) were then loaded onto the sample holder under inert atmosphere. The sample holder was moved to the instrument under argon, and the spectrum was collected at 25°C.

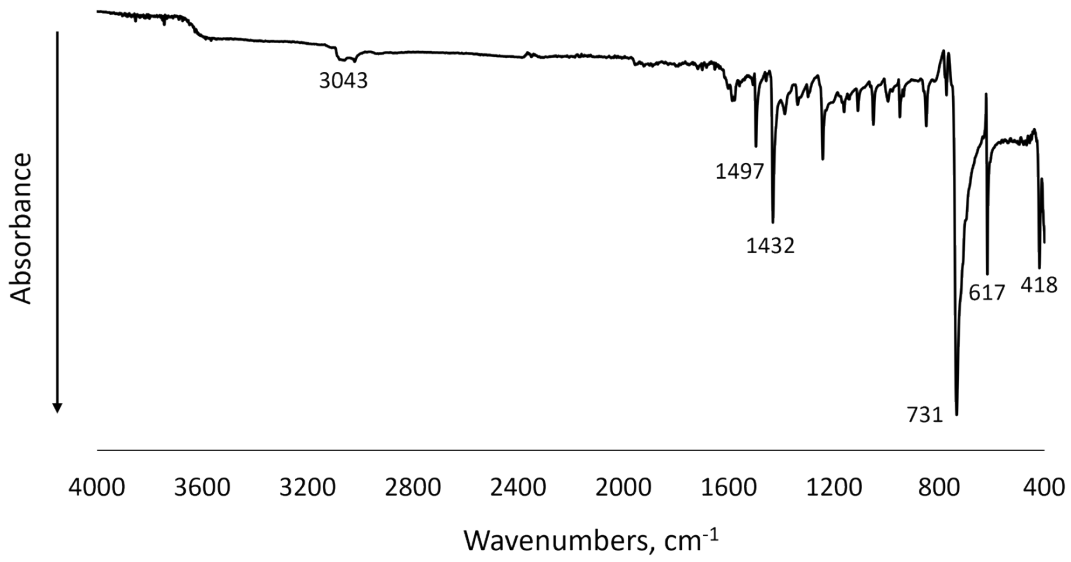

Fig. S9 ATR-IR spectrum of $[(C_{18}H_{12})_3]^{\bullet+}(Ga_3Cl_{10})^-$ (collected on a Shimadzu IRTracer-100 Fourier Transform Infrared Spectrometer QATR10 Single Reflection ATR accessory).

V. Computational methods

We conducted density functional theory (DFT) calculations to analyze the interactions between triphenylene (TP) monomers in π-stacking configurations. Geometry optimizations were carried out at the (U)M05-2X[14]/6-311G(d) level of theory for all molecules and finite aggregates. The unrestricted (U) formalism was applied specifically to open-shell systems when necessary. The choice of this DFT level is made based on previous thorough investigations.[15,16] The initial geometries were derived from isolated segments of the crystal structure $[(C_{18}H_{12})_3]^{\bullet+}(Ga_3Cl_{10})^-$ first reported here. To confirm the reliability of these geometrical optimizations, we checked for the absence of imaginary frequencies in all stationary points. Molecular calculations were carried out using the Gaussian 16 program.[17] Gibbs free energies (ΔG) were evaluated in the gas phase, with unscaled vibrational frequencies. To analyze the electrostatic potential-based atomic charges, we employed the CHELPG method as implemented in Gaussian 16.[18] For the calculation of total interaction energy ($\Delta E_{int,n}^{q}$) and average interaction energy per pair (ΔE_{pair}^{q}) between triphenylenes in the $[(C_{18}H_{12})_n]^q$ columns of triphenylenes we employed the following equations:

$$\Delta E_{int,n}^{q} = E_{\mathbf{[(C18H12)nq]}} - E_{\mathbf{[(C18H12)1q]}} - (n-1)\times E_{\mathbf{[(C18H12)]}} \quad \text{..... (eq. S1)}$$

$$\Delta E_{pair}^{q} = \Delta E_{int,n}^{q}/(n-1) \quad \text{..... (eq. S2)}$$

Here, q denotes the total charge of the TP column, and n indicates the number of TP monomers in the column. $E_{\mathbf{[(C18H12)nq]}}$ and $E_{\mathbf{[(C18H12)]}}$ refer to the total energy of a cluster (aggregate) with n units with charge q and a neutral monomer, respectively. All computed finite cluster energies refer to fully relaxed optimized geometries. A limited number of different q values were considered in the computational modeling in order to obtain insights into the charge dependency of the intermolecular interactions.

Further insights into the charge distribution among the TPs were obtained through CHELPG charge analysis for the isolated molecules and aggregates system[18] generating the factional charges on each TP in various aggregates listed as Q_i values. Accordingly,

$$q = \sum_{i}^{n} Q_i \text{.....} \ (eq.S3)$$

where the summation is extended over the aggregate of *n* TP molecules. The average interplanar distances (d_{av}) between the individual TPs in the $[(C_{18}H_{12})_n]^+$ aggregates were calculated by averaging C···C short contact lengths using:

$$d_{av} = \sum_{i}^{m} \frac{d_i(C \cdots C)}{m} \quad \text{..... (eq. S4)}$$

In equation S4, d_i(C···C) values are the lengths of carbon-carbon short contacts between a TP pair and *m* is the number of short C···C contacts. Harmonic Oscillator Measure of Aromaticity (HOMA)[19] indexes are calculated for selected systems using Multiwfn code.[20]

The periodic boundary condition (PBC) calculations on the crystal structure provided a tool in addition to computations on aggregates. The unit cell comprising six TP units with a total charge of +2 and two $Ga_3Cl_{10}^-$ anions, was examined through these PBC calculations using the spin-polarized method to account for the radical nature of the TPs in this charge transfer salt. Furthermore, we used the PBE density functional,[21] a kinetic energy cut-off of 30 Ry, and norm-conserving pseudopotentials. All the PBC calculations were carried out using Quantum Espresso program v.7.1,[22] and the Visualizations of the optimized structures, orbital, and spin densities were generated using the VESTA software.[23] The inclusion of magnetic effects in the periodic calculations was managed using the 'nspin=2' setting in Quantum Espresso. Bader charge analysis for the unit cells in the PBC computations[24] were also analyzed by eq. (S4).

VI. Validation of Charge Distributions in $[(C_{18}H_{12})_3]^{+1}$

Table S5: Charge distribution using various models for the triphenylene trimeric cluster

$[(C_{18}H_{12})_3]^{+1}$ Fragment	CHELPG charges	NPA charges	Mulliken charges	Hirshfeld charges
TPA	0.19	0.21	0.23	0.24
TPB	0.62	0.58	0.54	0.52
TPC	0.19	0.21	0.23	0.24

VII. Size dependency of the interaction energy in π-stacking aggregates of TP cation radical columns

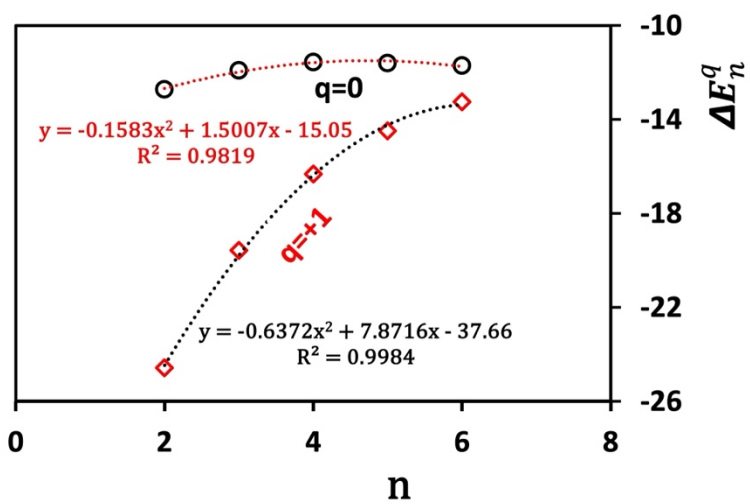

Fig. S10 Variation in interaction energy (ΔE_n^q) vs (n) associated with adding a triphenylene to $[(C_{18}H_{12})_{n-1}]^q$. Red diamonds represent the mono-cationic cluster (q=+1), and black circles denote the corresponding neutral cluster (q=0).

VIII. HOMA analysis

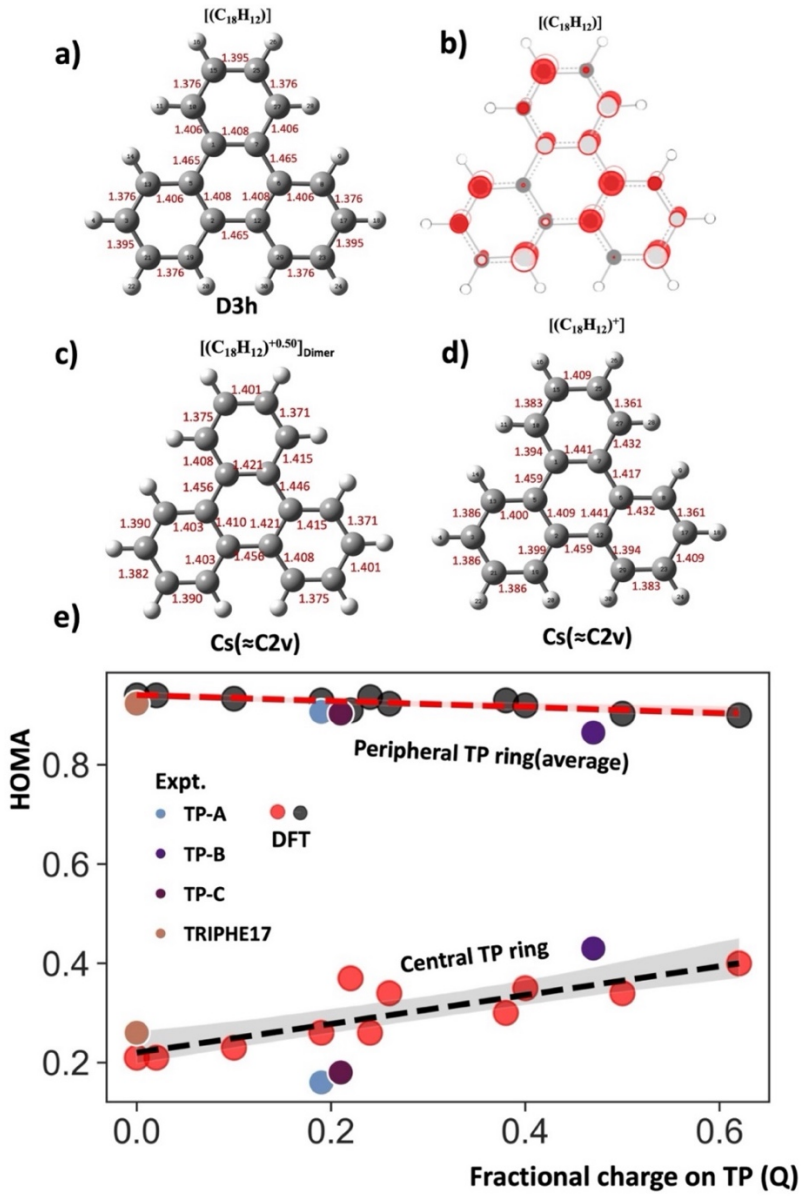

Fig. S11 (a) Optimized structure of neutral triphenylene (TP) and the C-C bond length, (b) Hückel level HOMO of the neutral TP monomer. (c) Structure and C-C bond lengths of TP carrying a fractional charge of +0.5, derived from the optimization of its +1 charged dimer. (d) Optimized structure of +1 charged TP monomer and its C-C bond distances. (e) Variation of harmonic oscillator model of aromaticity (HOMA) index as the fractional charge on TP changes. TRIPHE17 is the refcode of neutral TP in the Cambridge Structural Database.[25]

The HOMA analysis indicates that the aromaticity of the central ring is small while the peripheral rings are highly aromatic as was shown before for TP.[26] The fractional charge dependency is weak for both types of rings.

IX. Bond distance distribution in various positively charged TP cation radical aggregates

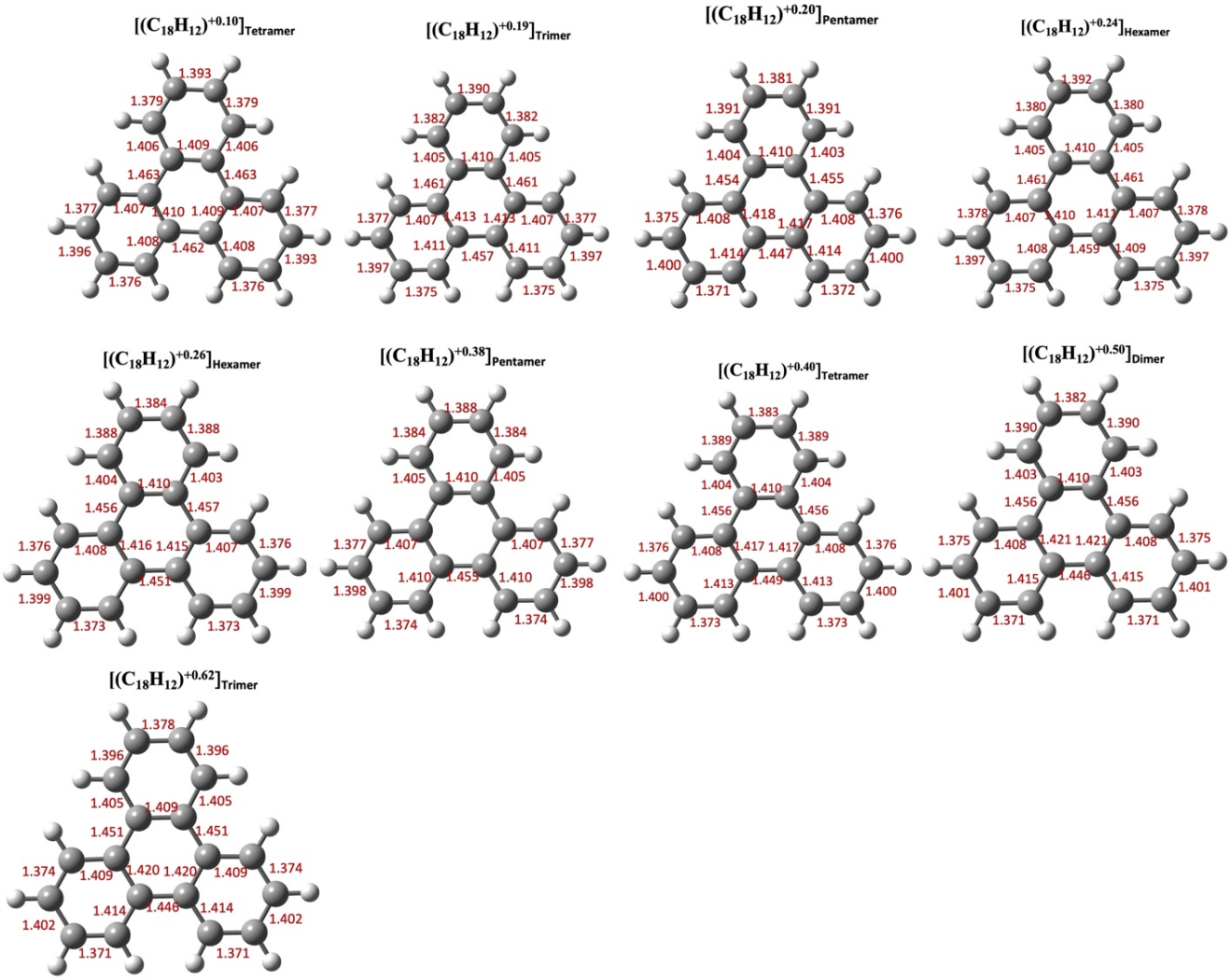

Fig. S12 Structure and C-C bond lengths of triphenylene carrying various fractional charges, derived from the optimization of its +1 charged column.

X. The effect of different isovalues for illustrating intermolecular overlap

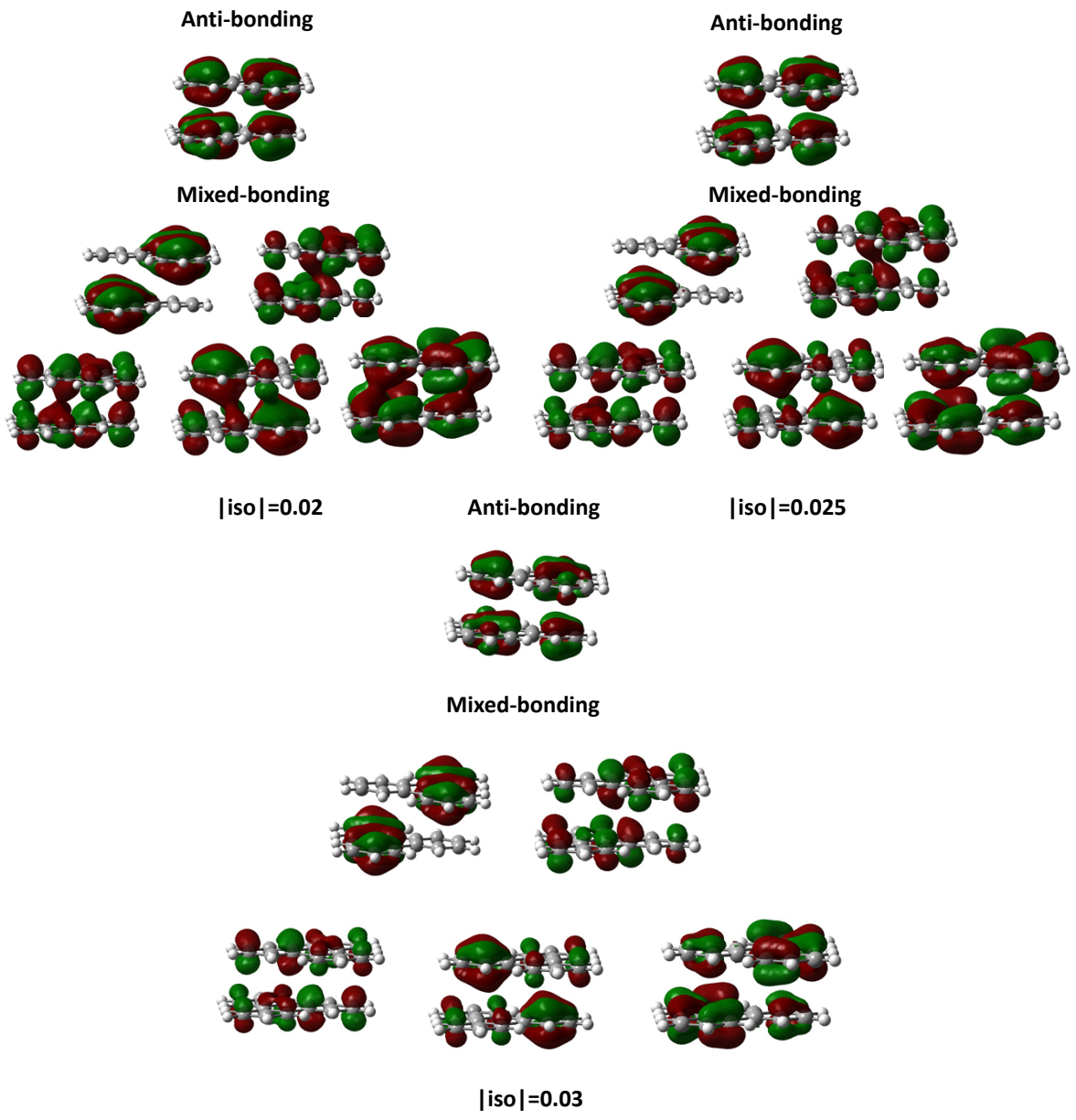

Fig. S13 Relevant orbitals of [(C18H12)2]+1 at various isosurface value.

XI. References

(1) N. V. Kozhemyakina, J. Nuss and M. Z. Jansen, *Für Anorg. Allg. Chem*., 2009, **635**, 1355–1361.
(2) SAINT; part of Bruker APEX3 software package (version 2018.7-2): Bruker AXS, 2018.
(3) SADABS; part of Bruker APEX3 software package (version 2018.7-2): Bruker AXS, 2018.
(4) G. M. Sheldrick, *Acta Crystallogr.* **2015**, *A71*, 3-8.
(5) G. M. Sheldrick, *Acta Crystallogr.* **2015**, *C71*, 3-8.
(6) O. V. Dolomanov, L. J. Bourhis, R. J. Gildea, J. A. K. Howard and H. Puschmann, *J. Appl. Crystallogr.*, 2009, **42**, 339-341.
(7) H. A. Oeye and W. Bues, *Acta. Chem. Scand. A.*, 1975, **A29**, 489-498.
(8) S. Ulvenlend, L. Bengtsson-Kloo and K. Ståhl, *J. Chem. Soc., Faraday Trans.*, 1995, **91**, 4223-4234.
(9) S. Ulvenlund, A. Wheatley and L. A. Bengtsson, *J. A,. Chem. Soc., Chem. Commun*, 1995, **1**, 59-60.
(10) J. Åkerstedt, R. Zaffaroni and L. Kloo, *Dalton Trans.*, 2010, **39**, 8132-8134.
(11) M. Gorlov, A. Fischer and L. Kloo, *Angew. Chem. Int. Ed.*, 2005, **44**, 3906-3908.
(12) D. Freudenmann and C. Feldmann,. *Dalton Trans.*, 2011, **40**, 452-456.
(13) P. Coburger, F. Masero, J. Bösken and V. Mougel, *Angew. Chem. Int. Ed.*, 2022, **61**, e202211749.
(14) Y. Zhao, N. E. Schultz and D. G. Truhlar, *J. Chem. Theory Comput.*, 2006, **2**, 364-382.
(15) R. Bhattacharjee, H. Jervis, M. E. McCormack, M. A. Petrukhina and M. Kertesz, *J. Am. Chem. Soc.*, 2024, **146**, 10465-10477.
(16) Z. Mou, Y.-H. Tian and M. Kertesz, *Phys. Chem. Chem. Phys.*, 2017, **19**, 24761-24768.
(17) M. J. Frisch, G. W. Trucks, H. B. Schlegel, G. E. Scuseria, M. A. Robb, J. R. Cheeseman, G. Scalmani, V. Barone, G. A. Petersson, H. Nakatsuji, X. Li, M. Caricato, A. V. Marenich, J. Bloino, B. G. Janesko, R. Gomperts, B. Mennucci, H. P. Hratchian, J. V. Ortiz, A. F. Izmaylov, J. L. Sonnenberg, D. Williams-Young, F. Ding, F. Lipparini, F. Egidi, J. Goings, B. Peng, A. Petrone, T. Henderson, D. Ranasinghe, V. G. Zakrzewski, J. Gao, N. Rega, G. Zheng, W. Liang, M. Hada, M. Ehara, K. Toyota, R. Fukuda, J. Hasegawa, M. Ishida, T. Nakajima, Y. Honda, O. Kitao, H. Nakai, T. Vreven, K. Throssell, J. A. Montgomery, Jr., J. E. Peralta, F. Ogliaro, M. J. Bearpark, J. J. Heyd, E. N. Brothers, K. N. Kudin, V. N. Staroverov, T. A. Keith, R. Kobayashi, J. Normand, K. Raghavachari, A. P. Rendell, J. C. Burant, S. S. Iyengar, J. Tomasi, M. Cossi, J. M. Millam, M. Klene, C. Adamo, R. Cammi, J. W. Ochterski, R. L. Martin, K. Morokuma, O. Farkas, J. B. Foresman, and D. J. Fox, Gaussian 16, Revision A. 03, Gaussian. Inc., Wallingford CT, 2016.
(18) C. M. Breneman and K. B. Wiberg, *J. Comput. Chem.*, 1990, **11**, 361-373.
(19) J. Kruszewski and T. Krygowski, *Tetrahedron Lett.*, 1972, **13**, 3839-3842.
(20) T. Lu and F. Chen, *J. Comput. Chem.*, 2012, **33**, 580-592.
(21) J. P. Perdew, K. Burke and M. Ernzerhof, *Phys. Rev. Lett.*, 1996, **77**, 3865-3868.
(22) P. Giannozzi, S. Baroni, N. Bonini, M. Calandra, R. Car, C. Cavazzoni, D. Ceresoli, G. L. Chiarotti, M. Cococcioni and I. Dabo, *J. Phys.: Condens. Matter*, 2009, **21**, 395502.
(23) K. Momma and F. Izumi, *J. Appl. Crystallogr.*, 2008, **41**, 653-658.
(24) G. Henkelman, A. Arnaldsson and H. Jónsson, *Comput. Mater. Sci.*, 2006, **36**, 354-360.
(25) A. Li, F. Li, Y. Chen, Y. Xie, X. Li, X. Liu, S. Xu, W. Xu, J. Wang and Z. Li, *ACS Mater. Lett.*, 2022, **4**, 2151-2158.
(26) T. M. Krygowski and H. Szatylowicz, *ChemTexts,* 2015, **1**, 1-10.